

# Spinal curvature measurement by tracked ultrasound snapshots

**Tamas Ungi<sup>1</sup>, Franklin King<sup>1</sup>, Michael Kempston<sup>2</sup>, Zsuzsanna Keri<sup>1</sup>, Andras Lasso<sup>1</sup>,  
Parvin Mousavi<sup>3</sup>, John Rudan<sup>2</sup>, Daniel P. Borschneck<sup>2</sup>, Gabor Fichtinger<sup>1</sup>**

<sup>1</sup>Laboratory for Percutaneous Surgery, School of Computing, Queen's University, Kingston, Canada

<sup>2</sup>Department of Surgery, School of Medicine, Queen's University, Kingston, Canada

<sup>3</sup>Medical Informatics Laboratory, School of Computing, Queen's University, Kingston, Canada

Corresponding author:

**Tamas Ungi, MD, PhD**

Adjunct Assistant Professor

School of Computing, Queen's University

557 Goodwin Hall, Kingston, ON, Canada, K7L 2N8

Tel: 1-613-483-3122

Fax: 1-613-533-6513

E-mail: [ungi@cs.queensu.ca](mailto:ungi@cs.queensu.ca)

## Abstract

Monitoring spinal curvature in adolescent kyphoscoliosis requires regular radiographic examinations; however, the applied ionizing radiation increases the risk of cancer. Ultrasound imaging is favorable over X-ray because it does not emit ionizing radiation. Therefore, we tested an ultrasound system for spinal curvature measurement, with the help of spatial tracking of the ultrasound transducer. Tracked ultrasound was used to localize vertebral transverse processes as landmarks along the spine to measure curvature angles. The method was tested in two scoliotic spine models by localizing the same landmarks using both ultrasound and X-ray imaging and comparing the obtained angles. Close correlation was found between tracked ultrasound and radiographic curvature measurement. Differences between results of the two methods were  $1.27 \pm 0.84^\circ$  (average  $\pm$  SD) in an adult model and  $0.96 \pm 0.87^\circ$  in a pediatric model. Our results suggest that tracked ultrasound may become a safer and more accessible alternative to radiographic spine monitoring in adolescent kyphoscoliosis.

## Keywords

Adolescent Idiopathic Kyphoscoliosis, Scoliosis, Kyphosis, Tracked sonography, Tracked ultrasound snapshot

## Introduction

Kyphoscoliosis affects approximately 1 in 1000 individuals and causes severe spinal deformity in about 10% of these cases (Goldman *et al.* 2012). About 90% of the cases in this disease are of the idiopathic type. They are discovered in adolescent age (10-14 years), and progress until the spine reaches full development (age of 16-22 years). Kyphoscoliosis progression is monitored by quantitative measurement of the spinal curvature (Stokes *et al.* 1994) and treatment decisions are based on angles measured during monitoring. The curvature is most commonly quantified by the Cobb angle, defined between a line drawn parallel to the end-plates of vertebrae above and below the curvature. Cobb angle below 20° requires only monitoring; Cobb angle between 20° and 40° can be treated by bracing to slow progression. Surgical treatment is advised when Cobb angle exceeds 40° or when respiratory problems occur due to severe chest deformation.

The standard diagnostic and progression monitoring method of kyphoscoliosis is radiographic examination, exposing the patient to ionizing X-ray radiation. But repeated radiographic examinations are linked to an increased risk of breast cancer development in girls with scoliosis (Hoffman *et al.* 1989; Doody *et al.* 2000). A more recent study found that X-ray diagnostics in the childhood significantly contributes also to leukemia and prostate cancer (Schmitz-Feuerhake *et al.* 2011). This risk increases with cumulative radiation dose, and estimated to reach twofold compared to the baseline population risk.

Various technologies have been investigated in the past for radiation-free evaluation of scoliosis. Surface topographical methods estimate the spine curvature from scanning the patient's skin with a stereo camera, but they are not sufficiently precise, cannot assess vertebral rotation, and cannot visualize the bone architecture (Goldberg *et al.* 2001). A recent surface topographic study reported difference of up to 9° compared to radiographic Cobb angle measurement (Frerich *et al.* 2012). Special magnetic resonance imaging (MRI) machines offers accurate and safe evaluation of the spinal curves in a standing patient

position, but MRI is more expensive and less accessible compared to other modalities (Diefenbach *et al.* 2013). Furthermore, MRI is not compatible with metallic implants, and requires the patient to be motionless for several minutes. Ultrasound imaging provides safe visualization of the posterior surface of the spine, and it is more accessible than MRI or X-ray. Portable ultrasound machines would allow spine monitoring even in areas with no permanent medical imaging devices. A significant linear correlation was discovered between the radiographic Cobb angle and the vertebral rotation measured by ultrasound at the apical vertebra in untreated patients (Suzuki *et al.* 1989). This is a safe and real-time method to estimate spinal curvature (Li *et al.* 2010), but the correlation is relatively weak and in patients with commenced treatment correlation is not observable anymore. Therefore, vertebral rotation measurement is not suitable for routine scoliosis monitoring. Another application of ultrasound imaging equips the transducer with position tracking. This opens new possibilities in ultrasound diagnostics, because a 3-D volume from tracked 2-D ultrasound images can be reconstructed. The reconstructed volumes reveal vertebral landmarks that enable measurement of spinal deformations (Purnama *et al.* 2010). In vitro experiments confirm that visible laminae could be used as landmarks to estimate the Cobb angle (Chen *et al.* 2011). Tracked ultrasound images can be used not only for reconstruction of 3-D volumes, but to define anatomical landmarks in the 3-D tracking space. Tracked ultrasound snapshots (TUSS) technique uses recorded 2-D ultrasound images with spatial tracking information, and they have been successfully applied for spinal interventions (Ungi *et al.* 2012). Zheng and Cheung proposed a method equivalent to TUSS to localize vertebral landmarks along the spine, and measure scoliosis angles by lines connecting these landmarks (Zheng and Cheung 2011). However, their method requires a wide ultrasound transducer to capture both sides of vertebrae in images in axial orientation. None of the ultrasound-based techniques have been translated to clinical practice yet.

We investigated tracked ultrasound snapshots in sagittal orientation for spinal curvature measurement using transverse processes as vertebral landmarks. A commercially available tracked ultrasound system

with a standard linear transducer was used with freely available open-source software. We evaluated the accuracy of this method on two scoliotic spine models by comparing measurements to conventional radiographic measurements. Tests were done by three different operators to assess reproducibility.

## **Materials and methods**

### **Experiment design**

Vertebral angles measured by tracked ultrasound were evaluated by comparing them to angles determined on X-ray images, which are considered clinical standard in spinal curvature monitoring. All vertebra angles were measured relative to a reference line that was defined by averaging the angles of all vertebrae. Measurement of each vertebra relative to this reference line provided 17 samples (12 thoracic and 5 lumbar) in each phantom for our comparative study. The reference line is also not sensitive to errors in individual vertebral angles; therefore other vertebrae do not contribute to the error in measured angle of each vertebra.

Each vertebra orientation was measured by the transverse process angle (TxA), defined by a line between the lateral ends of the two transverse processes (Figure 1) relative to the reference line. TxA was chosen for our measurements because it can be directly visualized in both ultrasound and X-ray images. The most common radiographic landmarks used in scoliosis measurement are end-plates of vertebrae (Figure 1), because they are clearly visible in human radiographs. However, end-plates are not visible on ultrasound images due to the acoustic shadowing from posterior anatomical structures. TxA was clearly visible in radiographs, so the comparison between sonographic and radiographic modalities could be reliably made in this study using TxA.

Three physicians acted as operators and performed all measurements independently for inter-operator variability analysis. All operators were experienced in radiographic analysis of spine curvatures. Radiographic images for ground truth measurements were acquired using a GE Brivo XR (GE Healthcare, Waukesha, WI, USA) X-ray system.

All operators were asked to identify the two end-plates and also measure the TxA on radiographic images for each vertebra. Then, all operators performed the sonographic measurement protocol on the spine phantoms so the comparison of TxA measurements could be done between the two modalities. We evaluated inter-operator variability of sonographic TxA measurement against radiographic end-plate angle measurement, since end-plate angle is considered as the current clinical standard in spine curvature measurement.

### **Tracked sonography system**

The tracked ultrasound measurement system consisted of a conventional ultrasound machine, a position tracker, and a data acquisition computer (Figure 2). A position sensor was rigidly fixed to the ultrasound transducer, and another position sensor (reference sensor) was attached to the patient's back to provide a reference coordinate system for position tracking. The reference sensor was placed in a plastic holder with anatomical direction marks so the system could show the acquired ultrasound images in an anatomical coordinate system for easier analysis of sonographic landmarks. We used an ultrasound machine integrated with an electromagnetic position tracker, Sonix Tablet with GPS extension (Ultrasonix, Richmond, BC, Canada). This product integrates a Model 180 electromagnetic tracking sensor (Ascension, Milton, VT, USA) in the housing of the ultrasound transducer. According to data given by the manufacturer, this sensor is tracked within a radius of 580 mm from the electromagnetic field generator with a static orientation error of 0.5° RMS (root mean square) and position error of 1.4 mm RMS. The GPS extension also exposes open tracker ports on the tracker system control unit (SCU), allowing us to add the

reference sensor to the system. Ultrasound images and tracking data were processed and saved on a separate computer to reduce the computation load of the ultrasound machine.

Data processing software of the tracked sonography system was modularly designed for convenient adaptation to different ultrasound machines and tracker systems (Figure 3).

Software interface to the hardware components was provided by the Public Software Library for Ultrasound Research (PLUS)<sup>1</sup> (Lasso *et al.* 2012). PLUS provided temporal synchronization between the imaging and tracking data, and provided calibration for accurate ultrasound image tracking. The processed tracked ultrasound data was sent by PLUS through the OpenIGTLink network communication protocol (Tokuda *et al.* 2009) to the end user application. The end user application was implemented as a downloadable extension for the 3D Slicer application framework<sup>2</sup>. It also used modules of the SlicerIGT extension<sup>3</sup>. 3D Slicer is a medical image processing, analysis, and visualization software that facilitates the development of new prototype applications in the form of extensions (Fedorov *et al.* 2012). The software that we implemented and used for this study can be installed from the extension manager of the latest version of the 3D Slicer application. The name of the extension is Scoliosis. All software used in this study is open-source, freely available for research or commercial use without any restrictions.

## Experimental phantom models

Scoliotic phantom models were used for the evaluation of sonographic spine curvature measurement compared to conventional radiographic measurement. All tests were done on two phantom models, an

---

<sup>1</sup> [www.plustoolkit.org](http://www.plustoolkit.org)

<sup>2</sup> [www.slicer.org](http://www.slicer.org)

<sup>3</sup> [www.slicerigt.org](http://www.slicerigt.org)

adult (Item# 1323-21, Sawbones, Vashon, WA, USA), and a pediatric spine (Item# 1323-30, Sawbones, Vashon, WA, USA). The spine models were treated with X-ray contrast material on the surface by the manufacturer for radiographic imaging. We placed them in gelatine gel to enable ultrasound imaging. Photos of the phantoms were taken before placing them in acoustic gel. The photos are shown in Figure 4, along with their radiographs.

### **Sonography protocol**

Tracked ultrasound data was collected using an Ultrasonix L14-5GPS transducer (Ultrasonix, Richmond, BC, Canada), at a frequency of 5 MHz, and imaging depth of 60 mm. Imaging focus was set at 40 mm as a typical distance of transverse processes from the skin. Gain and dynamic range was adjusted by each operator to create clear visual contrast between bone surface reflections and background soft tissue. No filtering algorithms were applied on the images captured directly from the ultrasound machine. Standard water-based ultrasound gel was used for acoustic connection between the phantom and the transducer surface. Transverse processes in the spine were visible at similar imaging settings in both humans and phantom models (Figure 5).

### **Angle measurement protocol**

TxA of vertebrae were defined between midpoints of transverse processes as seen on cross sections in ultrasound images parallel to the spine (Figure 6). The lateral ends of the processes were scanned for consistent measurements. Two tracked ultrasound snapshots were taken for each vertebra for measurement of TxA. The transverse process midpoints were manually selected on these ultrasound snapshots.



To conveniently find paramedian planes for TxA, the midline of the spine was marked on the skin surface along spinous processes. The marked midline significantly reduced scanning time for curvature measurement, which may become an important factor because young patients may not be able to maintain a straight posture for an extended time. The total scanning time was under 2 minutes in all experiments.

TxA measurements were performed after sonographic data acquisition, using the *ruler* annotation tool and the *Scoliosis* module of the 3D Slicer application. Figure 7 shows sonographic TxA measurements in the measurement software. Recorded sonographic snapshots can be individually hidden from the visualization scene, so only the two snapshots of one vertebra are shown during measurement to avoid obstruction by other segments when defining individual TxA lines.

Radiographic measurements were done on postero-anterior radiographic images, by manually placing lines at the superior and inferior end-plates of each vertebra, and along the transverse processes (Figure 1).

## Statistical analysis

Inter-operator differences were computed by pairwise absolute difference between the three operators, and they are expressed as average  $\pm$  standard deviation of differences. To compare inter-operator differences between radiographic end-plate measurement and sonographic TxA, we used one-tailed independent samples T-test with Bonferroni correction for repeated experiments (adult and pediatric). The comparison of sonographic TxA and radiographic TxA was done using linear correlation. Absolute differences between corresponding measurements from the two modalities were also expressed as average  $\pm$  standard deviation.

## Results

Average inter-operator differences are summarized in Figure 8. The inter-operator difference was significantly lower with sonographic measurement compared to radiographic end-plate angle measurement, which is the current clinical standard in spinal curvature assessment.

Correlation of sonographic and radiographic angles is shown in Figure 9. The correlation coefficient computed from all sonographic TxA with radiographic TxA by all operators is  $R=0.998$  in the adult phantom and  $R=0.997$  in the pediatric phantom. The differences between sonographic and radiographic TxA were  $1.27\pm 0.84^\circ$  in the adult model and  $0.96\pm 0.87^\circ$  in the pediatric model. The maximum difference between the two methods was  $3.4^\circ$ .

## Discussion

Inter-operator difference in sonographic TxA measurement was lower than in radiographic measurements. This suggests that sonographic TxA is a repeatable method to measure spinal curvature. In our comparison between sonographic and radiographic TxA, we found a very strong correlation between the two modalities. This indicates that sonographic spinal curvature measurement may be as reliable as the conventional radiographic method.

The main limitation of our experiment was that the phantom models were rigid, unlike patients who may move and change the curvature of their spine during ultrasound imaging. After gaining experience in sonographic TxA measurement, our operators completed the full scanning process within two minutes. Most adolescents can maintain a straight standing posture for this long period of time. If additional support is needed for younger patients, an assistant may hold the patients' shoulders from the sides

during imaging without interfering with their postures. Final proof of practical usability, however, can only be achieved by a future clinical study.

Another important technical limitation reported by our operators is that sonographic landmarks of the transverse processes should be defined manually at each spinal segment. Landmarking happens off-line after the scan. If all vertebral segments are analyzed, it may take up to six minutes for one patient. This time could be reduced in follow-up cases when the segments characterizing the main curvatures of the spine are already identified and other segments may be omitted. Future image processing development may also enable automatic vertebra recognition, completely eliminating the need for manual landmark definitions.

It has been shown using MRI that a significant proportion of vertebra rotation in scoliosis is due to the plastic deformation within the vertebrae themselves, not only the deformation of the discs (Birchall *et al.* 2005). This suggests that the Cobb angle thresholds defined in current clinical protocols by the angle of end-plates may not be directly applicable to TxA values, since the end-plates may deform relative to the transverse processes. If TxA measurement will be introduced in clinical practice, therapeutic recommendations may be established only after patient follow-up studies. Therefore, TxA cannot immediately replace conventional Cobb angle measurement in the near future.

Tracked ultrasound measurement has a number of potential advantages compared to conventional radiography. The increased risk of cancer development in children monitored by X-ray imaging may be lowered to the baseline population level. The cost of installation and the footprint of tracked ultrasound systems are only a fraction compared to the radiography systems. This may facilitate wider accessibility and lower the cost of patient follow-up in adolescent kyphoscoliosis. Finally, tracked sonographic measurement provides vertebra landmark points in 3-D space; therefore it allows vertebra rotation angle

measurement besides scoliotic curvature measurement. This additional information on spinal deformity may prove to be useful in risk assessment and therapeutic decision making in the future.

Our experiments were done using an electromagnetic position tracker. Although the tracking field is sufficiently large for scanning an adult spine, the signal-noise ratio decreases as the tracking sensor moves away from the field generator. Therefore, optical position tracking of the ultrasound transducer may seem to be a more suitable alternative, especially when electromagnetic noise can be present in the examination room. However in our experiments, TxA accuracy compared to radiographic ground truth did not depend on distance from the field generator, which suggests that the currently available commercial tracked ultrasound systems using electromagnetic tracking are also suitable for sonographic scoliosis monitoring.

Although many different metrics were developed and studied in the past decades, computerized automatic measurement of spinal deformities remains a challenging task (Vrtovec *et al.* 2009). Our sonographic method is still dependent on the operator selecting landmarks for TxA definition. However, the number of user interactions in tracked sonographic curvature measurement is comparable to radiographic methods. Low inter-operator variability found in our study also suggests that tracked ultrasound could become a reliable diagnostic and monitoring tool in scoliosis. In comparison, radiographic methods also have significant limitations (Kim *et al.* 2010). The variability in radiographic Cobb-angle measurement is reported to be 2-7° (Malfair *et al.* 2010, Sardjono *et al.* 2013). The angle measurement of the same curve is reported to increase by 5° in the afternoon compared to measurement in the morning (Beauchamp *et al.* 1993).

## **Conclusions**

We conclude that tracked sonographic TxA measurement is a promising method in kyphoscoliosis monitoring. If future human subject studies support our results, it may become the recommended modality over radiography due to its safety, reproducibility, portability, and low cost.

## **Acknowledgements**

Gabor Fichtinger is supported as a Cancer Care Ontario Research Chair.

## References

1. Beauchamp M, Labelle H, Grimard G, Stanciu C, Poitras B, Dansereau J. Diurnal variation of Cobb angle measurement in adolescent idiopathic scoliosis. *Spine (Phila Pa 1976)* 1993;18(12):1581–1583.
2. Birchall D, Hughes D, Gregson B, Williamson B. Demonstration of vertebral and disc mechanical torsion in adolescent idiopathic scoliosis using three-dimensional MR imaging. *Eur Spine J*. 2005 Mar;14(2):123-9.
3. Chen W, Lou EH, Le LH. Using ultrasound imaging to identify landmarks in vertebra models to assess spinal deformity. *Conf Proc IEEE Eng Med Biol Soc*. 2011;2011:8495-8.
4. Diefenbach C, Lonner BS, Auerbach JD, Bharucha N, Dean LE. Is radiation-free diagnostic monitoring of adolescent idiopathic scoliosis feasible using upright positional magnetic resonance imaging? *Spine (Phila Pa 1976)*. 2013 Apr 1;38(7):576-80.
5. Doody MM, Lonstein JE, Stovall M, Hacker DG, Luckyanov N, Land CE. Breast cancer mortality after diagnostic radiography: findings from the U.S. Scoliosis Cohort Study. *Spine (Phila Pa 1976)*. 2000 Aug 15;25(16):2052-63.
6. Fedorov A, Beichel R, Kalpathy-Cramer J, Finet J, Fillion-Robin JC, Pujol S, Bauer C, Jennings D, Fennessy F, Sonka M, Buatti J, Aylward S, Miller JV, Pieper S, Kikinis R. 3D Slicer as an image computing platform for the Quantitative Imaging Network. *Magn Reson Imaging*. 2012 Nov;30(9):1323-41.
7. Frerich JM, Hertzler K, Knott P, Mardjetko S. Comparison of radiographic and surface topography measurements in adolescents with idiopathic scoliosis. *Open Orthop J*. 2012;6:261-5.

8. Goldberg CJ, Kaliszer M, Moore DP, Fogarty EE, Dowling FE. Surface topography, Cobb angles, and cosmetic change in scoliosis. *Spine (Phila Pa 1976)*. 2001 Feb 15;26(4):E55-63.
9. Goldman L, Schafer AI. *Goldman's Cecil medicine*, 24<sup>th</sup> edition. Elsevier Saunders, Philadelphia, PA, 2012. Page 605.
10. Hoffman DA, Lonstein JE, Morin MM, Visscher W, Harris BS 3rd, Boice JD Jr. Breast cancer in women with scoliosis exposed to multiple diagnostic x rays. *J Natl Cancer Inst*. 1989 Sep 6;81(17):1307-12.
11. Kim H, Kim HS, Moon ES, et al. Scoliosis imaging: What radiologists should know. *Radiographics*. 2010;30:1823-1842.
12. Lasso A, Heffter T, Pinter C, Ungi T, Fichtinger G. Implementation of the PLUS open-source toolkit for translational research of ultrasound-guided intervention systems. *The MIDAS Journal - Medical Imaging and Computing*. <http://hdl.handle.net/10380/3363> (2012)
13. Li M, Cheng J, Ying M, Ng B, Zheng YP, Lam TP, Wong WY, Wong MS. Application of 3-D ultrasound in assisting the fitting procedure of spinal orthosis to patients with adolescent idiopathic scoliosis. *Stud Health Technol Inform*. 2010;158:34-7.
14. Malfair D, Flemming AK, Dvorak MF, et al. Radiographic evaluation of scoliosis: review. *AJR Am J Roentgenol* 2010;194(3 suppl):S8–S22.
15. Purnama KE, Wilkinson MH, Veldhuizen AG, van Ooijen PM, Lubbers J, Burgerhof JG, Sardjono TA, Verkerke GJ. A framework for human spine imaging using a freehand 3D ultrasound system. *Technol Health Care*. 2010;18(1):1-17.
16. Sardjono TA, Wilkinson MH, Veldhuizen AG, van Ooijen PM, Purnama KE, Verkerke GJ. Automatic Cobb Angle Determination from X-ray Images. *Spine (Phila Pa 1976)*. 2013 Jun 21.

17. Schmitz-Feuerhake I, Pflugbeil S. 'Lifestyle' and cancer rates in former East and West Germany: the possible contribution of diagnostic radiation exposures. *Radiat Prot Dosimetry*. 2011 Sep;147(1-2):310-3.
18. Stokes IA. Three-dimensional terminology of spinal deformity. A report presented to the Scoliosis Research Society by the Scoliosis Research Society Working Group on 3-D terminology of spinal deformity. *Spine (Phila Pa 1976)*. 1994 Jan 15;19(2):236-48.
19. Suzuki S, Yamamuro T, Shikata J, Shimizu K, Iida H. Ultrasound measurement of vertebral rotation in idiopathic scoliosis. *J Bone Joint Surg Br*. 1989 Mar;71(2):252-5.
20. Tokuda J, Fischer GS, Papademetris X, Yaniv Z, Ibanez L, Cheng P, Liu H, Blevins J, Arata J, Golby AJ, Kapur T, Pieper S, Burdette EC, Fichtinger G, Tempany CM, Hata N. OpenIGTLink: an open network protocol for image-guided therapy environment. *Int J Med Robot*. 2009 Dec;5(4):423-34.
21. Ungi T, Abolmaesumi P, Jalal R, Welch M, Ayukawa I, Nagpal S, Lasso A, Jaeger M, Borschneck DP, Fichtinger G, Mousavi P. Spinal needle navigation by tracked ultrasound snapshots. *IEEE Trans Biomed Eng*. 2012 Oct;59(10):2766-72.
22. Vrtovec T, Pernus F, Likar B. A review of methods for quantitative evaluation of spinal curvature. *Eur Spine J*. 2009 May;18(5):593-607.
23. Zheng YP, Cheung CW. Three-dimensional (3D) ultrasound imaging; system for assessing scoliosis. United States Patent Application Publication. US 2011/0021914 A1.



## Figure legends

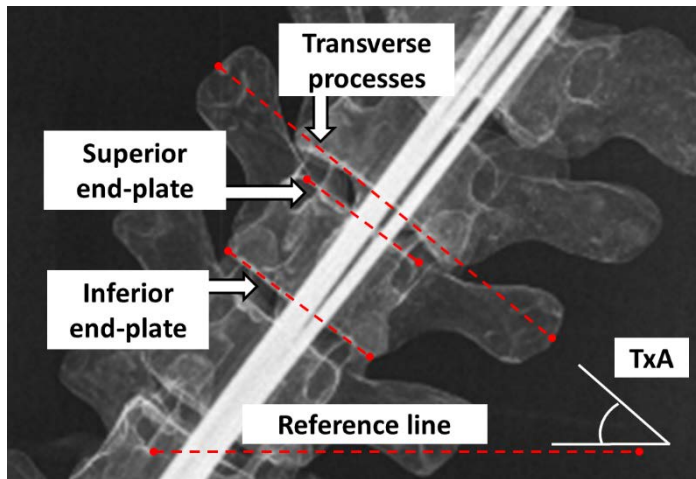


**Figure 1.** Radiographic lines used for curvature measurement for a single thoracic vertebra in postero-anterior radiographic projection.

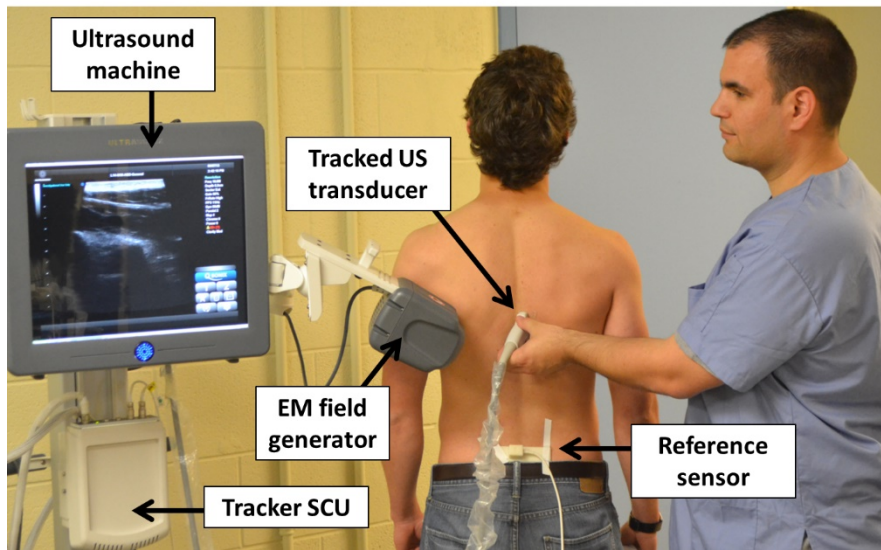
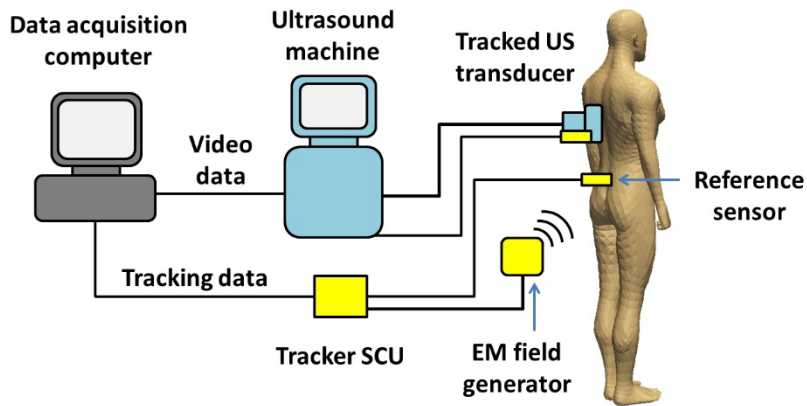


**Figure 2.** Schematics of a typical tracked sonography system (top image). The electromagnetic tracker consists of a system control unit (SCU) and an electromagnetic (EM) field generator. The tracking sensors and the field generator are connected to the tracker SCU. The bottom image shows the tracked sonographic system in use.

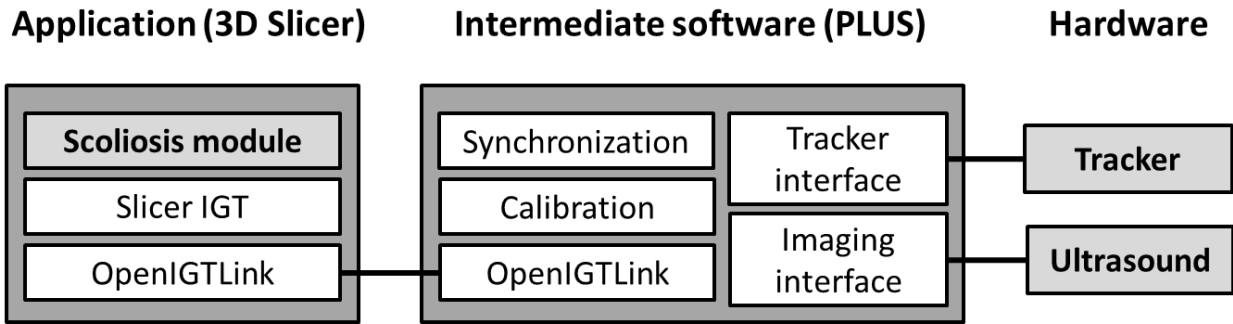


**Figure 3.** Software architecture overview of the scoliosis evaluation application.

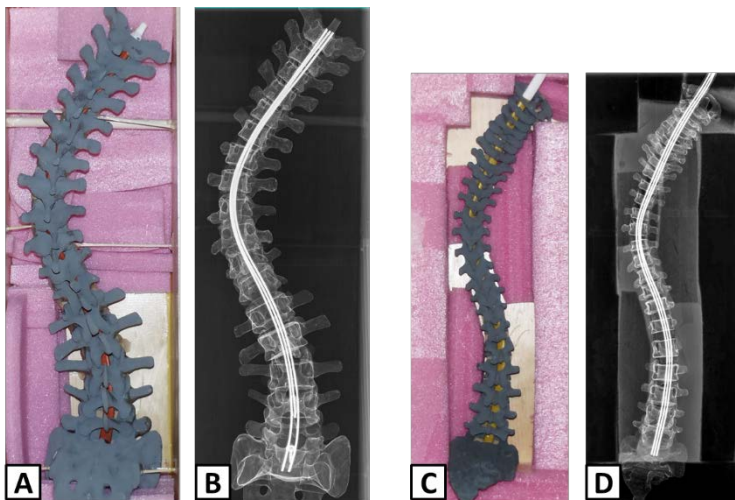


**Figure 4.** Experimental phantom models of an adult (A) and pediatric (C) scoliotic spine before placing them in acoustic gel. Their radiographic images (B and D) are also shown.

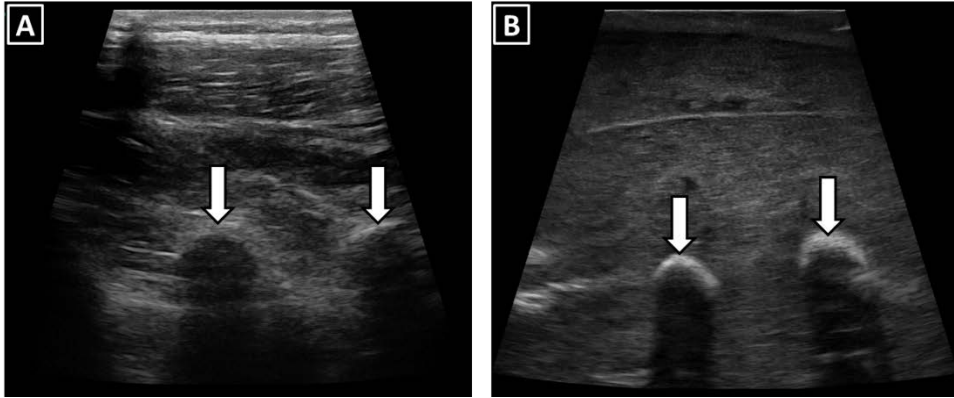


**Figure 5.** Paramedian ultrasound images of a human spine (A) and a phantom spine model (B). Arrows point at spinal transverse processes.

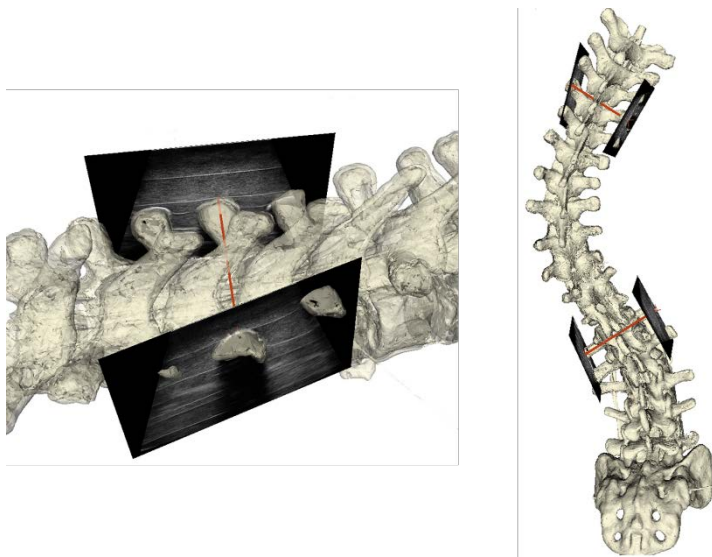


**Figure 6.** Illustration of TxA measurement. Left image shows ultrasound snapshots taken on both sides of a vertebra, and the sonographic landmarks connected for TxA definition. Image on the right shows two TxA lines for the major curvature of this spine model. Surface models for this illustration were generated from a CT scan, and they are not present in the actual measurement software.

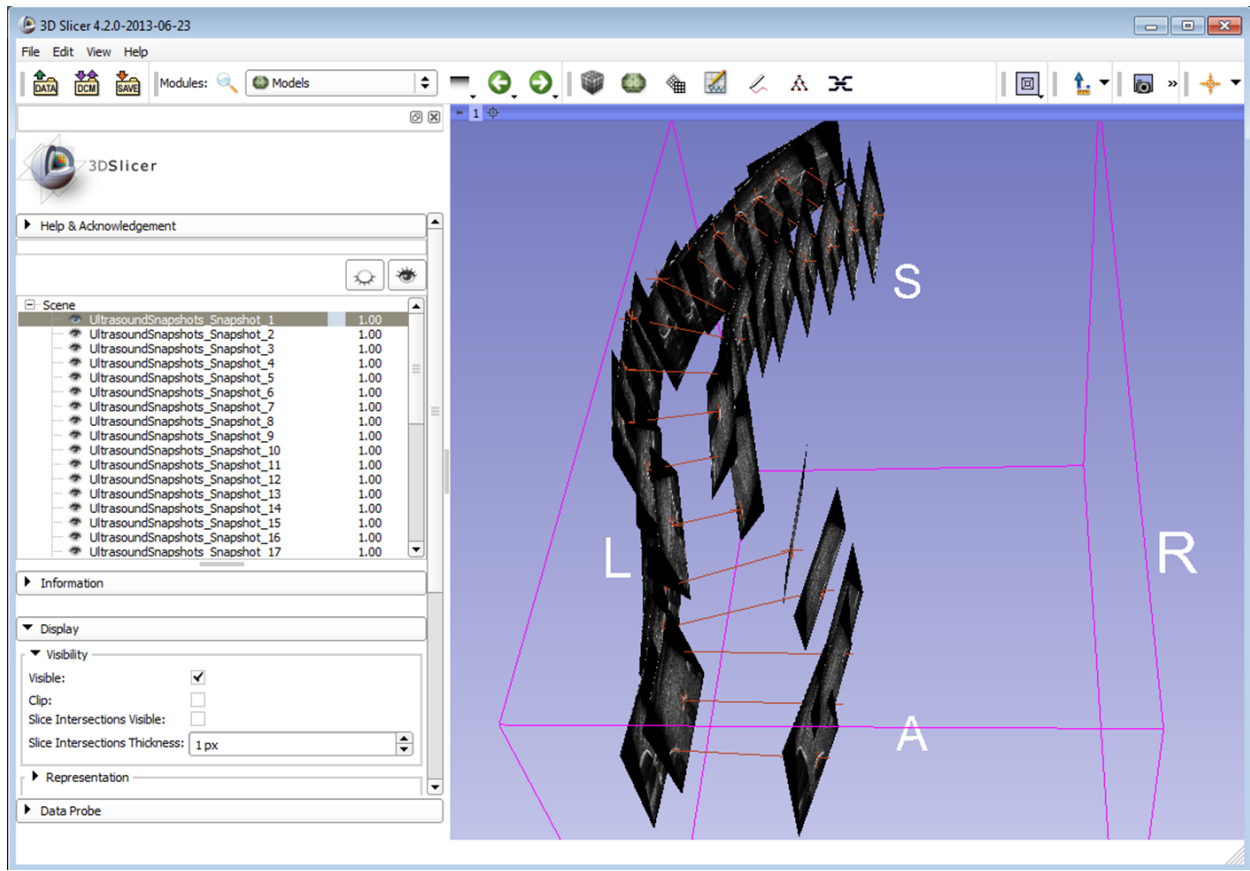


**Figure 7.** User interface of application for spinal curvature measurement. Image shows TxA lines and ultrasound snapshots for all segments of the adult spine model.

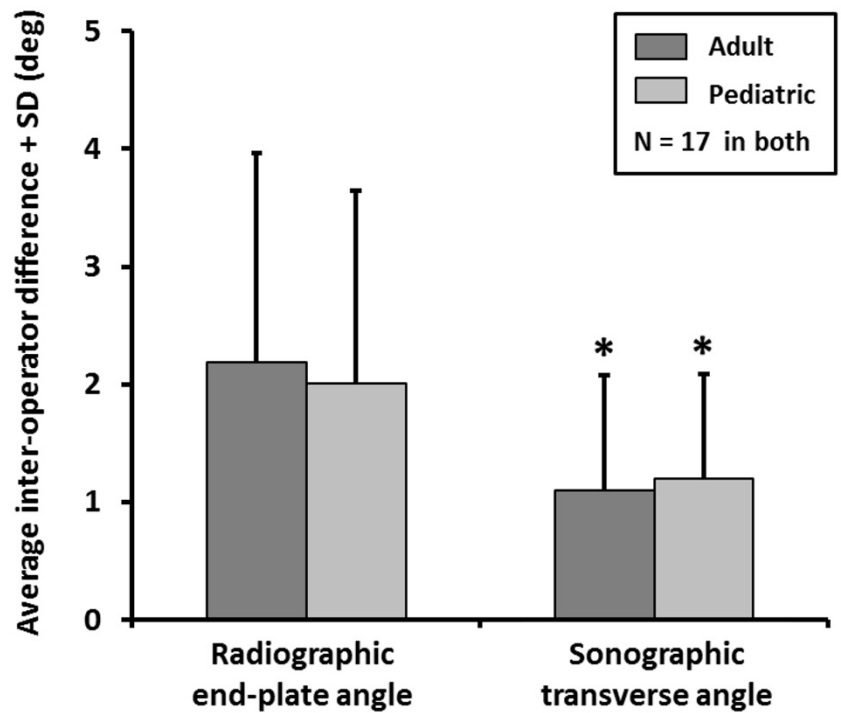


**Figure 8.** Average inter-operator difference of radiographic and sonographic TxA measurement. \*  $p < 0.05$  vs. radiographic measurement.

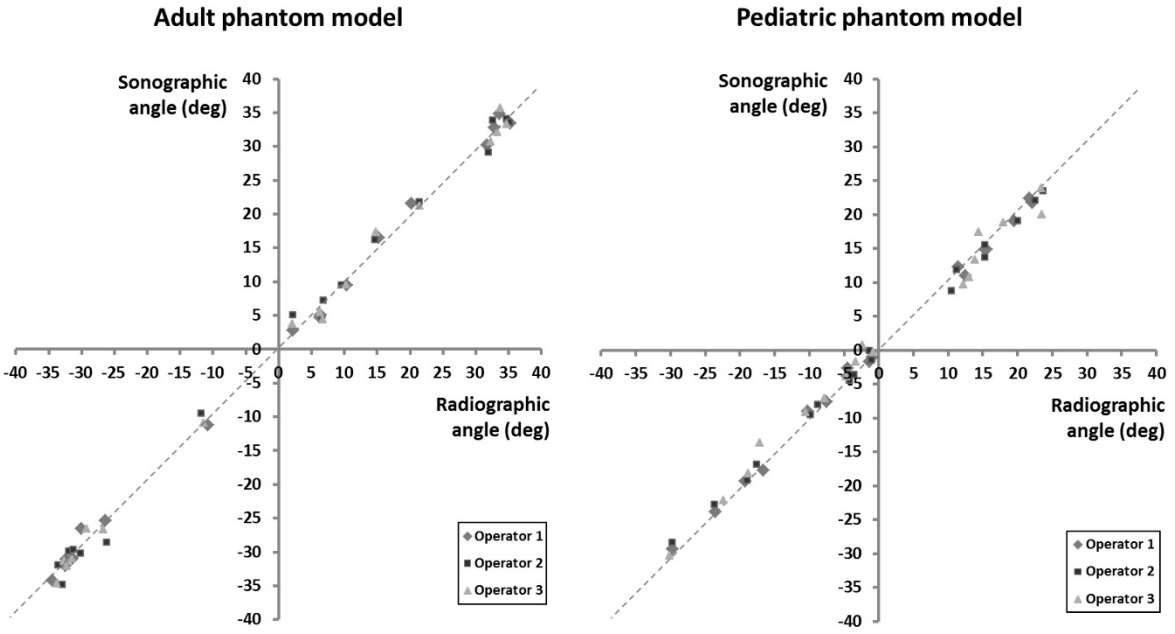


**Figure 9.** Scatterplot of sonographic TxA (vertical axis) vs. radiographic TxA (horizontal axis) in the adult model (first diagram) and the pediatric model (second diagram). Measurements of different operators are marked by different glyphs. Ideal correlation is marked by dashed line on both diagrams.